the Ni(II)–Ni(II) distance of 3.245 Å in bis(dimethylglyoximato)nickel(II)[43] supports the premise that if a *weak* positive kind of metal–metal interaction is operative in bis(dimethylglyoximato)nickel(II), then it is probably operative in the trinuclear nickel(II) cation and dinuclear nickel(II) molecule as well, especially if low-lying excited electronic states are assumed to mix with the ground state.

To the extent that these nickel(II)–nickel(II) interactions have any important influence on the chemistry of the trinuclear nickel(II) cation, it may be expected that the electron density of the terminal Ni(II) atoms along the $z$ direction approximately normal to the four-coordinated $NiS_2N_2$ plane would be localized on the exterior side opposite from the center Ni(1) atom. Any significant localization of negative charge in the external $z$ direction should make this complex more susceptible to coordination with a Lewis acid.

**Acknowledgments.**—We are much indebted to both Professor D. H. Busch and Dr. D. C. Jicha for furnishing samples of the compound and for their interest in this work. The use of CDC 1604 computers both at the University of Wisconsin Computing Center (made available for partial financial support from NSF and WARF through the University Research Committee) and at the Oak Ridge National Laboratory Computing Center is gratefully acknowledged.

---

CONTRIBUTION FROM THE DEPARTMENT OF CHEMISTRY,
PRINCETON UNIVERSITY, PRINCETON, NEW JERSEY 08540

# Raman and Infrared Frequencies, Force Constants, and Bond Polarizability Derivatives for Trimethylplatinum Hydroxide, Chloride, and Iodide[1a]

BY P. ALAN BULLINER,[1b] VICTOR A. MARONI,[1c] AND THOMAS G. SPIRO

*Received December 10, 1969*

Raman and infrared spectra have been obtained for the tetrameric molecules $[(CH_3)_3PtX]_4$ where X = OH, Cl, and I. For the hydroxide and chloride, single-crystal Raman polarizations provide unambiguous determination of the symmetry species of the observed frequencies. Assignments to internal coordinates were made by intercomparisons of the spectra and comparisons with related molecules. Of particular interest is the observation in each case of a set of three strong low-frequency bands in the Raman spectrum, with frequency ratios close to those predicted for a tetrahedron of like atoms bound to one another in the "simple cluster" approximation. Normal-coordinate analyses were carried out using force fields containing a force constant for metal–metal interaction. Absolute Raman intensities were measured for the totally symmetric modes and used to calculate bond polarizability derivatives and estimate bond orders. The results indicate that bonds between the platinum atoms and the bridging X atoms are weak and highly ionic. The Raman intensities provide evidence for weak interaction between platinum atoms, which decreases with increasing internuclear distance along the series X = OH, Cl, and I. The force constants for Pt–Pt stretching decrease in the same order but are much larger than expected in relation to the weakness of the Pt–Pt interaction. The bonding pattern is similar to that found previously for the oxygen-bridged complexes $Bi_6(OH)_{12}^{6+}$, $Pb_4(OH)_4^{4+}$, and $Tl_4(OC_2H_5)_4$.

## Introduction

As part of a continuing study[2-8] of the vibrational spectra of bridged polynuclear metal complexes we have investigated the Raman and infrared spectra of the compounds $[(CH_3)_3PtX]_4$, where X = OH, Cl, I. Of particular interest was the possibility of observing and more completely characterizing the type of strong low-frequency lines found in the Raman spectra of $Bi_6(OH)_{12}^{6+}$,[2] $Pb_4(OH)_4^{4+}$,[3] and $Tl_4(OR)_4$.[4]

The crystal structure of trimethylplatinum hydroxide, $(CH_3)_3PtOH$, has recently been completely determined[9,10] and shows the presence of discrete tetrameric units, with the platinum atoms and hydroxyl oxygens arranged in interpenetrating tetrahedra. Three methyl groups are attached to each Pt atom in such a way as to preserve the $T_d$ symmetry of the molecule. This structure is shown in Figure 1. An analogous structure had been found previously for trimethylplatinum chloride,[11] although the carbon atoms were not located. A partial structure determination for the iodide[12] also shows the presence of this type of tetrameric unit, but indicates a slight reduction of the $T_d$ symmetry and a different

(1) (a) This investigation was supported by Public Health Service Grant GM-13498, from the National Institute of General Medical Sciences, and by National Science Foundation Grant GP-10122. (b) NASA Trainee, 1966–1969. (c) NASA Trainee, 1964–1966.
(2) V. A. Maroni and T. G. Spiro, *J. Amer. Chem. Soc.*, **88**, 1410 (1966).
(3) V. A. Maroni and T. G. Spiro, *ibid.*, **89**, 45 (1967).
(4) V. A. Maroni and T. G. Spiro, *Inorg. Chem.*, **7**, 193 (1968).
(5) V. A. Maroni and T. G. Spiro, *ibid.*, **7**, 183 (1968).
(6) V. A. Maroni and T. G. Spiro, *ibid.*, **7**, 188 (1968).
(7) P. A. Bulliner and T. G. Spiro, *ibid.*, **8**, 1023 (1969).
(8) F. J. Farrell, V. A. Maroni, and T. G. Spiro, *ibid.*, **8**, 2638 (1969).
(9) T. G. Spiro, D. H. Templeton, and A. Zalkin, *ibid.*, **7**, 2165 (1968).
(10) H. S. Preston, J. C. Mills, and C. H. L. Kennard, *J. Organometal. Chem.*, **14**, 447 (1968).
(11) R. E. Rundle and J. H. Sturdivant, *J. Amer. Chem. Soc.*, **69**, 1561 (1947).
(12) G. Donnay, L. B. Coleman, N. G. Krieghoff, and D. O. Cowan, *Acta. Crystallogr.*, **B24**, 157 (1968).

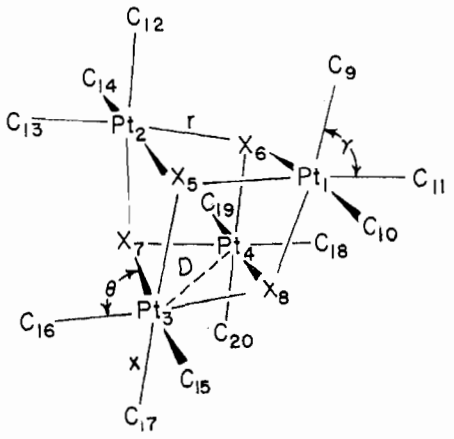


Figure 1.—The tetrameric structure of $[(CH_3)_3PtX]_4$ (X = OH, Cl, I) and suitable internal coordinates.

packing of the tetramers from that found for the hydroxide and chloride.

Several other workers[13-15] have reported on the vibrational spectra of these compounds, and some discrepancies in the earlier work have recently been corrected.[7,15b] We now report more complete vibrational data for the skeletal modes of all three compounds, based primarily on Raman spectra of single crystals. These vibrational data are used as the basis for normal-coordinate analyses and interpretation of the absolute Raman intensities, for comparison with previous results on the bismuth, lead, and thallium complexes mentioned.

## Spectra

Previous workers[13,15] have noted that the infrared spectra of $(CH_3)_3PtOH$, $(CH_3)_3PtCl$, and $(CH_3)_3PtI$ contain a large number of bands characteristic of the methyl group between 800 and 3000 $cm^{-1}$. Our Raman spectra show much the same pattern of frequencies, although only for the hydroxide has this region been investigated carefully. These vibrations, involving predominantly hydrogen motions, have very little effect on the vibrations of the $[C_3PtX]_4$ skeleton, which are expected to occur below 800 $cm^{-1}$. Since our interest is in these skeletal vibrations, the C–H vibrations are not discussed further.

For a molecule of $T_d$ symmetry, the active vibrations are of symmetry species $A_1$, E, and $T_2$. (Although trimethylplatinum iodide does not have strict $T_d$ symmetry in the crystal,[12] the Raman spectrum reveals no additional features or splittings attributable to the small distortions.) While all three species are Raman active, only $A_1$ vibrations give rise to polarized Raman lines in solution spectra, and only $T_2$ vibrations give rise to infrared bands. In principle then, it is possible to assign symmetry species to all observed frequencies from infrared and solution Raman spectra. This was not possible in the present case, however, since the number of infrared bands observed is less than required and since the limited solubility of the compounds reduces the number of distinct Raman lines which can be resolved in solution spectra.

Table I contains infrared frequencies between 200 and 800 $cm^{-1}$ for trimethylplatinum hydroxide and chloride and infrared frequencies between 60 and 800 $cm^{-1}$ for trimethylplatinum iodide. Table II contains solution Raman data for the hydroxide and iodide between 60 and 700 $cm^{-1}$.

TABLE I

INFRARED FREQUENCIES OBSERVED FOR $[(CH_3)_3PtX]_4$

| X = OH (200–800 $cm^{-1}$) | X = Cl (200–800 $cm^{-1}$) | X = I (60–800 $cm^{-1}$) |
|---|---|---|
| 724 vs | | |
| 592 w | 580 w | 562[b] w |
| 570[a] vw, sh | 572 w | |
| 396 sh | 223 s | 125 s |
| 369 vs | | 96 m |

[a] From ref 15a. [b] From ref 14.

TABLE II

RAMAN FREQUENCIES OBSERVED FOR $[(CH_3)_3PtX]_4$ IN SOLUTION (60–700 $cm^{-1}$)

| X = OH | X = I |
|---|---|
| 599 vs, p[b] | 567 vs, p |
| 592 vs, dp | 561 vs, dp |
| 433[a] w, p | 160 w, dp |
| 396[a] mw, dp | 125 w, dp |
| 353[a] mw, dp | 121 ms, p |
| 252[a] m, dp | 105 mw, dp |
| 137 ms, p | 87 m, p |
| 92 vs, dp | 63 vs, dp |

[a] In benzene; all others in carbon tetrachloride. [b] p = polarized, dp = depolarized.

Fortunately, another source of information is readily available for trimethylplatinum hydroxide and chloride because of their extremely simple crystal structures. The structure of each consists of one tetrameric molecule per primitive unit cell, and the point group, site group, and unit cell group are all $T_d$. Consequently no lattice vibrations are allowed in either the infrared or Raman spectra, and the internal vibrations retain the same symmetry properties in the crystal as in an isolated molecule.

The Raman tensors for the vibrations of a cubic crystal[16] are

$$A_1 \quad \begin{bmatrix} a & & \\ & a & \\ & & a \end{bmatrix} \qquad E \quad \begin{bmatrix} b & & \\ & b & \\ & & -2b \end{bmatrix} \begin{bmatrix} -\sqrt{3}b & & \\ & \sqrt{3}b & \\ & & \end{bmatrix}$$

$$T_2 \quad \begin{bmatrix} & d & \\ d & & \\ & & \end{bmatrix} \begin{bmatrix} & & \\ & & d \\ & d & \end{bmatrix} \begin{bmatrix} & & d \\ & & \\ d & & \end{bmatrix}$$

These tensors can be used to find orientations of the $E$ vectors of the incident and collected radiation for which vibrations of one or more of the symmetry species

(13) M. N. Hoechstetter, *J. Mol. Spectrosc.*, **13**, 407 (1964).

(14) L. A. Gribov, A. D. Gel'man, F. A. Zakharova, and M. M. Orlova, *Russ. J. Inorg. Chem.*, **5**, 473 (1960).

(15) (a) G. L. Morgan, R. D. Rennick, and C. C. Soong, *Inorg. Chem.*, **5**, 372 (1966); (b) D. E. Clegg and J. R. Hall, *J. Organometal. Chem.*, **17**, 175 (1969).

(16) R. Loudon, *Advan. Phys.*, **13**, 423 (1964).

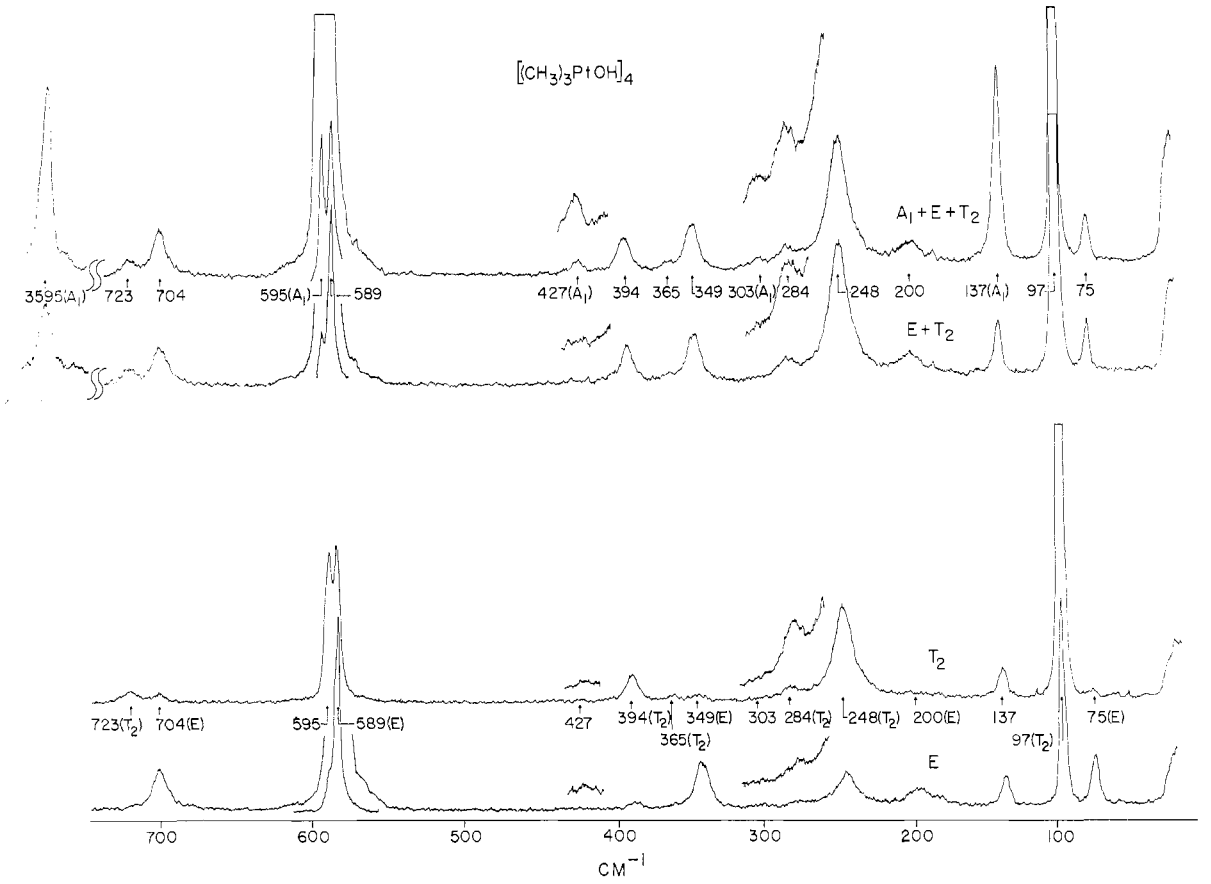


Figure 2.—Raman spectra of an oriented single crystal of $[(CH_3)_3PtOH]_4$. See text for details.

will give rise to zero intensity. A series of experiments using oriented single crystals can then be designed to permit the unambiguous assignment of a symmetry species to any observed Raman line on the basis of such absences.

The following set of experiments was found to be convenient to our Raman instrument (90° scattering) and the morphology of the crystals used (well-developed 101 faces). The crystal was aligned with its 101 ($x + z$) axis along the direction of the incident beam and its $10\bar{1}$ ($x - z$) axis along the collection direction. Four scans were then made as follows. (i) Incident radiation was polarized along $y$ and no analyzer was used; the tensor components involved were $yy$ and $xy + yz$. $A_1 + E + T_2$ vibrations were allowed to have nonzero intensity. (ii) Incident radiation was polarized along $x - z$ and no analyzer was used; the tensor components involved were $xy - yz$ and $xx - zz$. $E + T_2$ vibrations were allowed. (iii) Incident radiation was polarized along $x - z$, and scattered light was analyzed along $y$; the tensor components involved were $xy - yz$. $T_2$ vibrations are allowed. (iv) Incident radiation was polarized along $x - z$, and scattered light was analyzed along $x + z$; the tensor components involved were $xx - zz$. E vibrations were allowed.

The results for trimethylplatinum hydroxide (20–800 and 3550–3650 $cm^{-1}$) and trimethylplatinum chloride (20–650 $cm^{-1}$) are shown in Figures 2 and 3, respectively, each scan being labeled with the symmetry species of vibrations expected to be present. The changes in relative intensities between scans are easily sufficient to allow assignment of symmetry species to all observed lines. In every case where an independent check of the symmetry species is available from infrared or solution Raman data, the single-crystal determination is in accord. Table III contains the Raman frequencies and symmetry species observed for trimethylplatinum hydroxide between 800 and 3000 $cm^{-1}$ (not shown in Figure 2).

TABLE III

RAMAN FREQUENCIES AND SYMMETRY SPECIES OBSERVED FOR $[(CH_3)_3PtOH]_4$ BETWEEN 800 AND 3000 $CM^{-1}$

| | |
|---|---|
| 2969 ($T_2$) | 1284 ($A_1$) |
| 2900 ($A_1$) | 1247 (E) |
| 2829 ($A_1 + T_2$?) | 1174 (E) |
| 1431 ($T_2$) | 879 ($A_1$) |
| 1410 ($T_2$) | 857 ($T_2$) |

Figure 4 shows the single-crystal Raman spectrum of $(CH_3)_3PtI$. Attempts to observe polarization effects failed, although the crystal appeared to be of good quality. In view of the more complicated crystal structure of this compound, this experiment was not pursued further.

Table IV lists the observed frequencies between 20 and 800 $cm^{-1}$ for trimethylplatinum hydroxide, chloride, and iodide, with symmetry species in parentheses. For the hydroxide, the vibrations at 704 and 724 $cm^{-1}$ have been shown to involve primarily OH wagging[7,15b] and are of species E and $T_2$, respectively, as required.

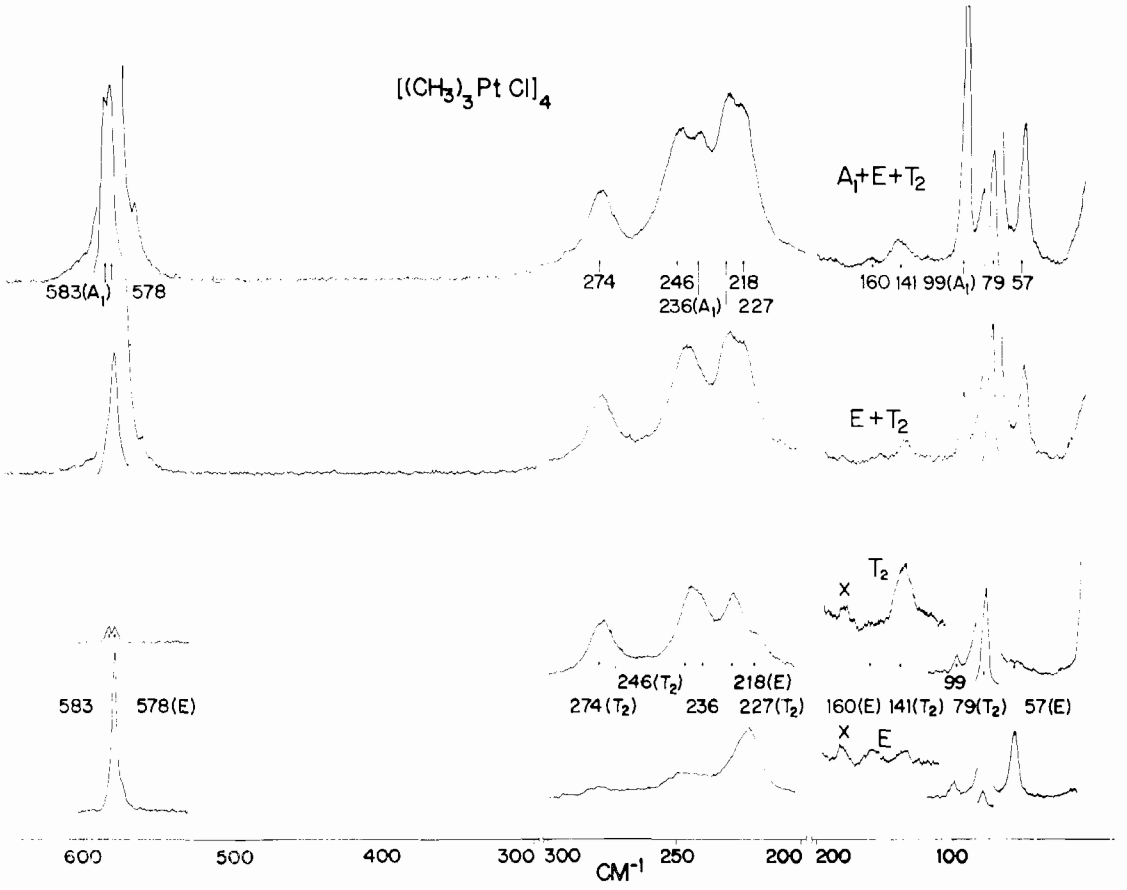


Figure 3.—Raman spectra of an oriented single crystal of $[(CH_3)_3PtCl]_4$. See text for details.

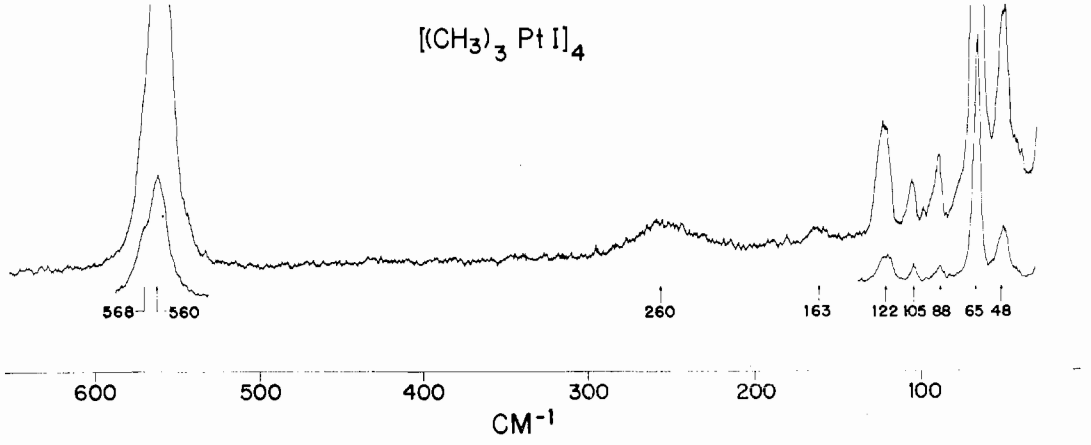


Figure 4.—Raman spectrum of a single crystal of $[(CH_3)_3PtI]_4$ (arbitrary orientation).

Neglecting both methyl and hydroxyl protons, the representation of the 17 active vibrations for these compounds is 4 $A_1$ + 5 E + 8 $T_2$. The unobserved frequencies for the hydroxide and chloride are then of species E + $T_2$ and $A_1$ + E + $T_2$, respectively. For the iodide, only 12 frequencies are observed, and the symmetry species of six of these is not directly determined.

## Assignments

The vibrational representations spanned by pertinent sets of internal coordinates are given in Table V. Qualitative assignments of the observed frequencies to the various types of internal coordinates are best made by comparing the spectra of the three compounds.

**Pt–C Stretching.**—The strong Raman lines and weak infrared bands found between 550 and 600 $cm^{-1}$ in all three compounds are readily assigned to Pt–C stretching vibrations by comparison with a large number of metal–methyl systems.[17] For the hydroxide and chloride, the four observed frequencies are in accord with the expected vibrational representation: $A_1$ + E + 2 $T_2$. The iodide spectra are very similar, but

(17) (a) D. M. Adams, "Metal-Ligand and Related Vibrations," St. Martin's Press, New York, N. Y., 1968, Chapter 4, and references therein; (b) D. E. Clegg and J. R. Hall, *Spectrochim. Acta, Part A*, **23**, 263 (1967).

TABLE IV

OBSERVED SKELETAL FREQUENCIES[a] FOR $[(CH_3)_3PtX]_4$ ($cm^{-1}$)

| | X = OH | X = Cl | X = I[d] |
|---|---|---|---|
| $\delta_{OH}$ | 724 ($T_2$) | | |
| | 704 (E) | | |
| $\nu_{Pt-C}$ | 595 ($A_1$) | 583 ($A_1$) | 568 ($A_1$) |
| | 592 ($T_2$) | 580 ($T_2$) | 562 ($T_2$) |
| | 589 (E) | 578 (E) | 560 |
| | 570[b] ($T_2$) | 572 ($T_2$) | *c* |
| $\nu_{Pt-X}$ + $\delta_{PtC_3}$ | 427 ($A_1$) | | |
| | 394 ($T_2$) | | |
| | 369 ($T_2$) | | |
| | 349 (E) | | |
| | | 274 ($T_2$) | |
| | 303 ($A_1$) | 246 ($T_2$) | |
| | 284 ($T_2$) | 236 ($A_1$) | 260 |
| | 248 ($T_2$) | 227 ($T_2$) | |
| | 200 (E) | 218 (E) | |
| | | 160 (E) | |
| | | 141 ($T_2$) | 163 |
| | | | 125 ($T_2$) |
| | | | 122 ($A_1$) |
| | | | 105 |
| | | | 96 ($T_2$) |
| $\nu_{Pt-Pt}$ | 137 ($A_1$) | 99 ($A_1$) | 88 ($A_1$) |
| | 97 ($T_2$) | 79 ($T_2$) | 65 |
| | 75 (E) | 57 (E) | 48 |

[a] Frequencies taken from solid-state Raman (Figures 2–4) and infrared (Table I) spectra. For those $T_2$ vibrations observed in both infrared and Raman, the frequencies given here are from the spectrum where the line is better resolved (and thus more accurately measured) or, if resolution is similar in both cases, averages of the two values. [b] There is some question as to whether this is a fundamental.[18a] [c] Uncertain shoulder (~550 $cm^{-1}$) in Raman spectrum not tabulated. [d] Symmetry species for X = I given only where these are unambiguously determined from ir or solution Raman work. Assignments for the other lines are discussed in text.

TABLE V

CONTRIBUTIONS OF INTERNAL-COORDINATE TYPES TO THE RAMAN AND INFRARED-ACTIVE NORMAL MODES OF $[C_3PtX]_4$

| | No. of contributions to each symmetry class | | |
|---|---|---|---|
| Internal coordinate | $A_1$ | E | $T_2$ |
| $x$, Pt–C bond str | 1 | 1 | 2 |
| $\gamma$, C–Pt–C angle bend | 1 | 1 | 2 |
| $r$, Pt–X bond str | 1 | 1 | 2 |
| $D$, Pt–Pt bond str | 1 | 1 | 1 |
| $\theta$, C–Pt–X angle bend | 1 | 2 | 3 |
| Total | 5 | 6 | 10 |
| Redundancies | 1 | 1 | 2 |

only one frequency is resolved in the infrared spectra. The line at 560 $cm^{-1}$ can be assigned E symmetry by analogy with the Raman spectra of the hydroxide and chloride.

**C–Pt–C Bending.**—Clegg and Hall[18] have assigned a medium-strength line at 259 $cm^{-1}$ in the Raman spectrum of $(CH_3)_3Pt(OH_2)_3^+$ to $PtC_3$ deformation modes. All three compounds under study here show medium-strength Raman lines in the range 200–310 $cm^{-1}$. For the hydroxide, the four Raman lines in this region are of the correct symmetry to be the expected $PtC_3$ deformation frequencies and are so assigned. For the chloride, the situation is more complicated, with the region between 140 and 280 $cm^{-1}$ containing a total of seven observed frequencies, which must include Pt–Cl stretching motions as well as $PtC_3$ deformation modes. The Raman spectrum of the iodide shows a very broad feature peaked at 260 $cm^{-1}$ with a weaker line at 163 $cm^{-1}$, and, as in the case of the hydroxide, the infrared spectrum shows no absorption in this region. Comparison of frequencies and intensities with those of the hydroxide suggest that the 260-$cm^{-1}$ line is of $T_2$ symmetry and the 163-$cm^{-1}$ line is of E symmetry. The second $T_2$ and the $A_1$ $PtC_3$ deformations are presumably covered by the stronger 260-$cm^{-1}$ line.

**Pt–X Stretching.**—Unlike the Pt–$C_3$ stretching and bending frequencies, the Pt–X stretching frequencies are expected to vary markedly among the three members of the series. For the hydroxide, the four frequencies between 340 and 430 $cm^{-1}$ are assigned to Pt–O stretching vibrations as discussed previously.[7] Neither the chloride nor the iodide shows vibrations in this region, which does however contain the frequency (357 $cm^{-1}$) assigned to Pt–O stretching in $(CH_3)_3Pt(OH_2)_3^+$.[18] The four vibrations assigned to Pt–O stretching are of the required symmetry species. In trimethylplatinum chloride, the Pt–Cl stretching vibrations are assigned in the region 140–300 $cm^{-1}$, along with the $PtC_3$ deformation modes. The seven frequencies observed for $(CH_3)_3PtCl$ in this region account for all but one of the modes expected for these two types of internal coordinates, the missing frequency corresponding to an $A_1$ vibration. For the iodide, the Pt–I stretching vibrations are assigned in the range 90–130 $cm^{-1}$. The frequencies at 125, 122, 105, and 96 $cm^{-1}$ can be assigned to symmetry species $T_2$, $A_1$, E, and $T_2$, respectively, on the basis of the infrared and solution Raman data.

**Cluster Modes.**—The remaining vibrational frequencies observed are in each case the three sharp lowest frequency Raman lines. These features are similar in appearance for the three compounds, although the frequencies decrease regularly from the hydroxide to the chloride to the iodide and the relative intensities differ somewhat. Similar features have previously been observed for $Bi_6(OH)_{12}^{6+}$,[2] in which an octahedral array of bismuth atoms is bridged by hydroxyl groups at the octahedron edges, and for $Pb_4(OH)_4^{4+}$ [3] and $Tl_4(OC_2H_5)_4$,[4] which have the same arrangement of metal atoms and bridging ligands as in $[(CH_3)_3PtX]_4$. The three Raman lines for the Bi, Pb, and Tl complexes were assigned[4–6] to stretching vibrations arising from metal–metal interactions. A simple model, neglecting both mixing of these modes with other vibrations of the molecule and interaction force constants involving the metal–metal coordinate, predicts three Raman frequencies in the ratio $2:\sqrt{2}:1$ for tetrahedral ($\nu_{A_1}:\nu_{T_2}:\nu_E$) or octahedral ($\nu_{A_{1g}}:\nu_{T_{2g}}:\nu_{E_g}$) arrangements of metal atoms. For the Bi, Pb, and Tl species, the observed frequency ratios are in good agreement with this prediction, and in each case

(18) D. E. Clegg and J. R. Hall, *Spectrochim. Acta, Part A*, **21**, 357 (1965).

the highest frequency mode was confirmed to be totally symmetric from solution Raman spectra. For the trimethylplatinum series, the frequency ratios observed are 2:1.41:1.09, 2:1.60:1.15, and 2:1.48:1.09 for the hydroxide, chloride, and iodide, respectively, and in the first two cases the single-crystal polarizations confirm the order $\nu_{A_1} > \nu_{T_2} > \nu_E$. By analogy, the two lowest cluster frequencies of trimethylplatinum iodide can be assigned, $T_2$ (65 $cm^{-1}$) > E (48 $cm^{-1}$).

**C–Pt–X Bending.**—This type of internal-coordinate spans the active vibrational representation $A_1 + 2\,E + 3\,T_2$. However, there are one $A_1$, one E, and two $T_2$ redundancy conditions through which changes in these angles can be expressed in terms of changes in C–Pt–C angles, Pt–X distances, and Pt–Pt distances, which have already been discussed. The remaining representation, $E + T_2$, describes changes in the orientation of rigid $PtC_3$ groups with respect to the rigid cage. It seems reasonable that such motions could have both low frequencies and low intensities, and it is assumed that the unobserved vibrations of species E and $T_2$ for both the hydroxide and the chloride are of this type.

## Normal-Coordinate Analyses

Normal-coordinate analyses were carried out on these molecules in order to obtain force constants for comparison with related complexes and in order to obtain eigenvectors for the calculation of bond polarizability derivatives from the Raman intensities. While normal-coordinate analyses on complicated molecules are necessarily approximate, the problem is less uncertain here than usual, in that for $[(CH_3)_3PtOH]_4$ all but two and for $[(CH_3)_3PtCl]_4$ all but three of the expected normal mode frequencies have been identified and assigned unambiguously to symmetry species, on the basis of their Raman polarizations.

For cyclic molecules, an inescapable ambiguity arises from redundancies of bond-stretching and angle-bending internal displacement coordinates. For the platinum tetramers a choice must be made between using Pt–Pt stretching coordinates or interior cage angle deformation coordinates, since either set is sufficient to describe the cluster vibrations. Since the lowest frequency Raman bands have frequency ratios close to those predicted by the simple cluster model, $\nu_{A_1}:\nu_{T_2}:\nu_E = 2:\sqrt{2}:1$, it is expected that a force field with Pt–Pt stretching will give a simpler fit to the spectra than a force field involving only interior angle bending, as was found[4-6] for $Bi_6(OH)_{12}^{6+}$, $Pb_4(OH)_4^{4+}$, and $Tl_4(OC_2H_5)_4$. Part of the object was in any case to compare force fields among these complexes, and we have therefore chosen to use a Pt–Pt force constant in the calculations.

The *G* matrices were calculated by the method of Wilson, *et al.*,[19] employing Schachtschneider's program GMAT.[20] The molecular parameters, listed in Table VI, were taken from the crystal structure determinations. The methyl groups and the hydroxyl groups were treated as point masses of mass 15 and 17, respectively. A general valence force field was used to construct the *F* matrices. Both *G* and *F* matrices were factored using symmetry coordinates generated from the internal coordinates by standard group theoretical methods.[19] Solution of the secular equation, with least-squares adjustment of the force constants, was accomplished with Schachtschneider's program FPERT.[20] The calculations proceeded in stages. Initial values of the diagonal valence force constants were chosen to calculate frequencies associated with the various internal coordinates in the spectral regions assigned in the preceding section. A minimum number of interaction force constants between internal coordinates of the same type was then introduced and the values were adjusted. This procedure yielded an acceptable, stable fit of the observed frequencies for the hydroxide. For the chloride, where the Pt–Cl stretching and C–Pt–C deformation modes occur in the same frequency region, the C–Pt–C bending force constants were transferred from the hydroxide calculation and the calculated frequencies were matched with the closest observed frequencies. Pt–Cl stretching force constants were then introduced and adjusted to fit the remaining frequencies. Final refinement of both the Pt–Cl and C–Pt–C force constants led to only small changes. For trimethylplatinum iodide, an interaction constant between Pt–I and Pt–Pt stretching coordinates was required to account for the two lowest $A_1$ frequencies. (For the heavy iodide bridging atoms, Pt–I and Pt–Pt modes are substantially mixed, and the simple cluster model breaks down.)

Since no frequencies assigned to predominantly C–Pt–X bending modes have been observed and no independent estimate of the associated force constant is available, this force constant was constrained to zero in the calculations described above. The effect of neglecting this force constant was subsequently examined for $[(CH_3)_3PtOH]_4$ by incrementally increasing its value from zero and readjusting the other nonzero force constants. There were perceptible effects on the Pt–O, Pt–Pt, and C–Pt–C force constants, and it became clear that inclusion of a significant value for the C–Pt–O bending force constant would require the introduction of additional interaction force constants to produce agreement with the observed cluster frequencies. Since there is no way to gauge the magnitude of

TABLE VI

GEOMETRIC PARAMETERS USED IN THE CONSTRUCTION OF *G* MATRICES FOR $[(CH_3)_3PtX]_4$

X = OH: Pt–O = 2.21 Å,[a] Pt–Pt = 3.42 Å,[a] Pt–C = 2.03 Å,[a] C–Pt–C = 87.5°[a]

X = Cl: Pt–Cl = 2.48 Å,[b] Pt–Pt = 3.73 Å,[b] Pt–C = 2.03 Å,[c] C–Pt–C = 87.5°[c]

X = I: Pt–I = 2.83 Å,[d] Pt–Pt = 4.00 Å,[d] Pt–C = 2.03 Å,[c] C–Pt–C = 87.5°[c]

[a] Average of values from re 9 and 10. [b] Reference 11. [c] Not determined in X-ray work; assumed to be the same as for X = OH. [d] Reference 12, ignoring apparent distortions from $T_d$ point symmetry.

(19) E. B. Wilson, J. C. Decius, and P. C. Cross, "Molecular Vibrations," McGraw-Hill, New York, N. Y., 1955.

(20) J. H. Schachtschneider, Technical Reports No. 231-64 and 57-65, Shell Development Co., Emeryville, Calif.

the C–Pt–O force constant, we chose to ignore it, recognizing that this uncertainty does limit somewhat the confidence to be placed in the calculated force constants.

### Discussion of Force Constants

The results of the normal-coordinate analyses are shown in Table VII, which gives the observed and calculated frequencies and the potential energy distribution. The final force constants are listed in Table VIII.

TABLE VII

RESULTS OF NORMAL-COORDINATE ANALYSES FOR $[(CH_3)_3PtX]_4$

| $\nu_{obsd}$, $cm^{-1}$ | $\nu_{calcd}$, $cm^{-1}$ | $V_{zz}$[a] | $V_{rr}$ | $V_{\gamma\gamma}$ | $V_{DD}$ | $V_{rD}$ |
|---|---|---|---|---|---|---|
| | | X = OH | | | | |
| 595 ($A_1$) | 598 | 95 | 3 | 1 | 1 | |
| 590 ($T_2$) | 590 | 99 | 1 | 0 | 0 | |
| 589 (E) | 588 | 99 | 0 | 0 | 0 | |
| 570 ($T_2$) | 570 | 97 | 2 | 0 | 0 | |
| 427 ($A_1$) | 423 | 4 | 88 | 5 | 3 | |
| 394 ($T_2$) | 398 | 2 | 96 | 1 | 1 | |
| 369 ($T_2$) | 370 | 1 | 97 | 2 | 0 | |
| 349 (E) | 347 | 0 | 99 | 0 | 0 | |
| 303 ($A_1$) | 308 | 0 | 7 | 91 | 2 | |
| 284 ($T_2$) | 279 | 0 | 3 | 96 | 1 | |
| 248 ($T_2$) | 242 | 0 | 1 | 99 | 1 | |
| 200 (E) | 208 | 0 | 0 | 99 | 1 | |
| 137 ($A_1$) | 135 | 0 | 2 | 3 | 94 | |
| 97 ($T_2$) | 100 | 0 | 1 | 2 | 97 | |
| 75 (E) | 76 | 0 | 0 | 1 | 99 | |
| ... (E) | 0 | | | | | |
| ... ($T_2$) | 0 | | | | | |
| | | X = Cl | | | | |
| 583 ($A_1$) | 581 | 99 | 1 | 0 | 1 | |
| 580 ($T_2$) | 580 | 99 | 1 | 0 | 0 | |
| 578 (E) | 576 | 100 | 0 | 0 | 0 | |
| 572 ($T_2$) | 576 | 100 | 0 | 0 | 0 | |
| ... ($A_1$) | 285 | 1 | 24 | 69 | 6 | |
| 274 ($T_2$) | 277 | 1 | 75 | 22 | 2 | |
| 246 ($T_2$) | 247 | 0 | 9 | 91 | 0 | |
| 236 ($A_1$) | 229 | 0 | 69 | 29 | 2 | |
| 225 ($T_2$) | 226 | 0 | 14 | 85 | 0 | |
| 218 (E) | 217 | 0 | 1 | 99 | 0 | |
| 160 (E) | 155 | 0 | 97 | 1 | 2 | |
| 141 ($T_2$) | 149 | 0 | 95 | 1 | 4 | |
| 99 ($A_1$) | 102 | 0 | 7 | 2 | 91 | |
| 79 ($T_2$) | 76 | 0 | 5 | 1 | 93 | |
| 57 (E) | 58 | 0 | 2 | 0 | 97 | |
| ... (E) | 0 | | | | | |
| ... ($T_2$) | 0 | | | | | |
| | | X = I | | | | |
| 568 ($A_1$) | 565 | 99 | 0 | 0 | 1 | 0 |
| 562 ($T_2$) | 564 | 99 | 0 | 0 | 0 | 0 |
| 560 (E) | 561 | 100 | 0 | 0 | 0 | 0 |
| ... ($T_2$) | 561 | 100 | 0 | 0 | 0 | 0 |
| ... ($A_1$) | 292 | 1 | 1 | 96 | 3 | −1 |
| 260 ($T_2$) | 260 | 0 | 1 | 98 | 1 | 0 |
| ... ($T_2$) | 202 | 0 | 1 | 98 | 1 | 0 |
| 163 (E) | 163 | 0 | 1 | 98 | 1 | 0 |
| 125 ($T_2$) | 124 | 0 | 97 | 2 | 14 | −13 |
| 122 ($A_1$) | 124 | 0 | 81 | 3 | 62 | −46 |
| 105 (E) | 101 | 0 | 98 | 2 | 17 | −16 |
| 96 ($T_2$) | 100 | 0 | 97 | 1 | 14 | −12 |
| 88 ($A_1$) | 89 | 0 | 29 | 0 | 47 | 24 |
| 65 ($T_2$) | 66 | 0 | 9 | 0 | 77 | 13 |
| 48 (E) | 48 | 0 | 5 | 0 | 86 | 8 |
| ... (E) | 0 | | | | | |
| ... ($T_2$) | 0 | | | | | |

[a] $V_{ij}$ is the normalized contribution to the potential energy from $F$-matrix elements of the type $F_{ij}$. The internal coordinates $x$, $r$, $\gamma$, and $D$ are defined in Figure 1.

TABLE VIII

FINAL FORCE CONSTANTS FOR $[(CH_3)_3PtX]_4$

| | X = OH | X = Cl | X = I |
|---|---|---|---|
| $f_r$[a] | 1.44 | 0.68 | 0.57 |
| $f_D$ | 0.79 | 0.50 | 0.49 |
| $f_x$ | 2.73 | 2.73 | 2.59 |
| $f_\gamma$ | 0.25 | 0.23 | 0.18 |
| $f_\theta$ | 0[b] | 0[b] | 0[b] |
| $f'_{rr}$(1–5, 2–5)[c] | 0.45 | 0.04 | 0.08 |
| $f''_{rr}$(1–5, 1–6) | 0.04 | 0.25 | 0[b] |
| $f'_{\gamma\gamma}$(9–1–10, 9–1–11) | 0.03 | 0.00 | 0.04 |
| $f''_{\gamma\gamma}$(9–1–10, 12–2–13) | 0.03 | 0.02 | 0.03[b] |
| $f'_{xx}$(1–9, 2–12) | 0.11 | 0[b] | 0[b] |
| $f'_{rD}$(1–5, 1–2) | 0[b] | 0[b] | −0.07 |

[a] All force constants in millidynes per angström. For $f_\gamma$, values were scaled to millidynes per ångström using Pt–C = 2.03 Å (see Table VI). [b] Constrained. [c] Numbers in parentheses indicate atoms defining the internal coordinates to which the interaction constants refer.

The Pt–C stretching force constants are well-defined, since the Pt–C vibrations are nearly pure, and their values, valid within the approximation of point-mass methyl groups,[21] are unremarkable, except that the slight decrease from the chloride to the iodide is apparently real. (For $(CH_3)_3PtBr$, preliminary infrared and Raman spectra show Pt–C stretching bands between 550 and 560 $cm^{-1}$, lower than either the chloride or the iodide.[22]) The C–Pt–C bending force constant is well determined for the hydroxide and the values for the chloride and iodide are reasonably consistent. The magnitude of this force constant is much larger for these molecules than for tetrahedral $M(CH_3)_4$ species,[21] consistent with the smaller angles in the present case.

The Pt–X stretching modes are quite pure for the hydroxide, but are appreciably mixed with C–Pt–C bending for the chloride, and with Pt–Pt stretching for the iodide. Consequently the associated force constants are less certain for the latter two molecules. The Pt–O primary stretching force constant has essentially the same value as the Tl–O constant[4] in the structurally analogous $Tl_4(OC_2H_5)_4$ (1.44 and 1.43 mdyn/Å, respectively). Evidently the Pt–O bonding is much more characteristic of a monovalent than of a tetravalent cation. The force constants are not strictly comparable, however, since no interaction constants were used in the $Tl_4(OC_2H_5)_4$ calculation, whereas the $[(CH_3)_3PtOH]_4$ calculation requires a substantial Pt–O stretch–stretch interaction constant at the oxygen atoms. While the magnitude of this interaction constant seems unusually large (30% of the primary Pt–O stretching force constant), no other reasonable set of force constants was found which could account for the unambiguously ordered set of four normal modes found in the Pt–O stretching region. Trimethylplatinum chloride also required a large Pt–Cl stretch–stretch

(21) R. K. Sheline, *J. Chem. Phys.*, **18**, 595, 602 (1950).
(22) V. A. Maroni and P. A. Bulliner, unpublished results.

interaction constant, and similar situations arose previously in normal-coordinate analyses of $Bi_6(OH)_{12}^{6+}$,[5] $Pb_4(OH)_4^{4+}$,[6] $Nb_6O_{19}^{8-}$,[8] and $Ta_6O_{19}^{8-}$.[8] Large interaction constants apparently express the complexity of the force fields in these highly condensed complexes.

The Pt–X primary stretching force constants in $[(CH_3)_3PtCl]_4$ and $[(CH_3)_3PtI]_4$ are smaller by a factor of about 3 than the force constants customarily associated with terminal metal–halogen bonds.[17a] The force constants suggest that each Pt–X linkage is worth on the order of one-third of a normal M–X bond, consistent with the halogen atoms bridging three platinum atoms each, although the work of Clegg and Hall[17b] indicates that part of the force constant lowering is due to the *trans* effect of the methyl groups. Hartley and Ware[23] determined an approximate stretching force constant of 1.1 mdyn/Å for the triply bridging chloride in the Mo(II) cluster complexes $(Mo_6Cl_8)X_6^{2-}$ (X = Cl, Br, I). The lower value of the Pt–Cl constant found here may again reflect a low effective Pt nuclear charge experienced by the bridging ligands, and the *trans* effect of the methyl groups.[15b]

Pt–Pt force constants are discussed in the following section in connection with the bond polarizability derivatives.

## Raman Intensities and Bond Polarizability Derivatives

Absolute Raman intensities were determined for the observed $A_1$ modes of the three $[C_3PtX]_4$ molecules, and these were converted to mean molecular polarizability derivatives, $\bar{\alpha}'_{Q_i} \equiv \partial\bar{\alpha}/\partial Q_i$, with the usual polarizability equation for freely rotating molecules[24]

$$I_{Qi} = \frac{KM(\nu_0 - \Delta\nu)^4}{\Delta\nu[1 - \exp(-h\Delta\nu/kT)]}(45)\left(\frac{6}{6 - 7\rho}\right)(\bar{\alpha}'_{Q_i})^2 \quad (1)$$

Here $K$ is an instrumental constant, $M$ is the molar concentration, $\nu_0$ is the exciting frequency, $\Delta\nu$ is the Raman shift, and $\rho$ is the depolarization ratio. This equation is applicable when no analyzer is used and depolarization ratios are determined by changing the direction of polarization of the incident laser beam. For totally symmetric vibrations of isotropic molecules in solution, $\rho = 0$.

Intensity measurements were made both in solution ($CCl_4$ and $CHCl_3$) and from the crystal spectra. For the cubic hydroxide and chloride crystals, the $A_1$ scattering tensor is isotropic (*i.e.*, $\rho = 0$). Since there is no evidence in the crystal structures for significant intermolecular effects (*e.g.*, hydrogen bonding), the molecular environments in the crystal and in an inert solvent should not be appreciably different. Consequently, for either molecule the intensities of the $A_1$ normal modes relative to one another should be quite similar in solution and crystal spectra. The data given for the hydroxide in Table IX support this assumption. While the crystal environment may have a small effect on the intensities, it is felt that the errors involved are less than errors arising from measurement of intensities from solution spectra, where resolution and signal-to-background ratios are much less favorable than in the crystal spectra. At least one intensity must however be measured in solution to provide an internal standard. For the hydroxide, the absolute value of $\bar{\alpha}'_Q$ (595 $cm^{-1}$) was determined by comparing the intensity of this line with that of $\nu_1(CCl_4)$ in a solution of known concentration. The value of $\bar{\alpha}'_{Q_1}(CCl_4)$ was taken as 0.686 $Å^2$ $(amu)^{-1/2}$, derived from the reported value of $\bar{\alpha}'_{C-Cl}$.[25] $\bar{\alpha}'_Q$ values for the other three $A_1$ lines of the hydroxide were then calculated from their intensities, relative to the 595-$cm^{-1}$ line, in crystal spectra. The same procedure was used to determine absolute $\bar{\alpha}'_Q$ values for the three $A_1$ lines of the chloride, except that the intensity of the 583-$cm^{-1}$ line was compared with $\nu_2$ of the solvent chloroform. $\bar{\alpha}'_{Q_2}$ ($CHCl_3$) was determined by measuring intensities for a mixture of $CHCl_3$ and $CCl_4$. For $[(CH_3)_3PtI]_4$ the solid and solution $A_1$ intensities were clearly incompatible. Since the crystals are monoclinic, the $A_1$ scattering tensor is not isotropic, so that it is impossible to relate the crystal intensities to $\bar{\alpha}'_Q$'s on the basis of the available data. Consequently, the solution intensities must be used for calculation of $\bar{\alpha}'_Q$ even though they are less accurately determined. The results of the intensity measurements are given in Table IX.

TABLE IX

$A_1$ INTENSITIES AND POLARIZABILITY DERIVATIVES FOR $[(CH_3)_3PtX]_4$

| X | $\nu$, $cm^{-1}$ | $R$[a] | $\bar{\alpha}'_Q$, $Å^2$ $(amu)^{-1/2}$ |
|---|---|---|---|
| OH | 595 | 4.82[b] ± 0.80[c] | 1.80 ± 0.15[e] |
| | 427 | 0.13 ± 0.05 (0.16)[d] | 0.23 ± 0.04 |
| | 303 | 0.13 ± 0.04 | 0.18 ± 0.03 |
| | 137 | 1.07 ± 0.40 (1.19)[d] | 0.27 ± 0.05 |
| Cl | 583 | 4.21[b] ± 0.70 | 1.62 ± 0.14 |
| | 236 | 0.22 ± 0.10 | 0.20 ± 0.05 |
| | 99 | 0.61 ± 0.15 | 0.16 ± 0.02 |
| I | 568 | 5.21[b] ± 1.61 | 1.71 ± 0.26 |
| | 122 | 0.59 ± 0.28 | 0.17 ± 0.04 |
| | 88 | 0.57 ± 0.27 | 0.13 ± 0.03 |

[a] $R$ is molar intensity, relative to $R[\nu_1(CCl_4)] = 1.00$, *i.e.*

$$R_i = \frac{I_i}{M_i}\frac{M_{CCl_4}}{I[\nu_1(CCl_4)]}$$

where the $I$'s have been corrected for instrument sensitivity. [b] Intensities of the hydroxide lines, relative to each other, and of the chloride lines, relative to each other, were obtained from crystal spectra, while analogous intensities for the iodide lines were obtained in $CCl_4$ solutions. For X = OH, intensities were placed on an absolute scale by measurement of $I(595)/I[\nu_1(CCl_4)]$. For X = Cl, $I(583)/I[\nu_2(CHCl_3)]$ and $I[\nu_2(CHCl_3)]/I[\nu_1(CCl_4)]$ were measured. [c] Estimated combined uncertainty in solute concentrations and intensity measurements. [d] Rough estimates from solution spectra. [e] Per cent errors in $\bar{\alpha}'_Q$ were taken to be half the per cent errors in $R$ ($\bar{\alpha}'_Q \propto I^{1/2}$), as uncertainties in other terms in eq 1 are small. Observed depolarization ratios were indistinguishable from the expected value of zero.

Normal mode mean polarizability derivatives can be transformed to mean polarizability derivatives

(23) D. Hartley and M. J. Ware, *Chem. Commun.*, 912 (1967).

(24) R. E. Hester in "Raman Spectroscopy," H. A. Szymanski, Ed., Plenum Press, New York, N. Y., 1967, Chapter 4.

(25) T. V. Long, II, and R. A. Plane, *J. Chem. Phys.*, **43**, 457 (1965).

assignable to the internal coordinates, $\bar{\alpha}'_u$, by solving the set of simultaneous equations[26]

$$\bar{\alpha}'_{Q_i} = \sum_j \sqrt{N_j}\, \bar{\alpha}'_{u_j} l_{ji} \qquad (2)$$

Here $N_j$ is the number of internal coordinates in the symmetry coordinate $S_j$, and $l_{ji}$ is the eigenvector element describing the displacement of $S_j$ in the normal mode $Q_i$. In the present case four $A_1$ normal modes are under consideration, corresponding to Pt–C, Pt–X, and Pt–Pt stretching and C–Pt–C bending. The eigenvectors, taken from the normal-coordinate analyses, are listed in Table X. Calculated values of

TABLE X

EIGENVECTORS FOR THE TOTALLY SYMMETRIC VIBRATIONS OF $[(CH_3)_3PtX]_4$ ($L_{A_1}$ MATRICES[a])

| | $Q_x$[b] | $Q_r$ | $Q_D$ | $Q_\gamma$ |
|---|---|---|---|---|
| | | X = OH | | |
| $S_x^{(A_1)}$ | 0.2653 | 0.0403 | 0.0035 | 0.0077 |
| $S_r^{(A_1)}$ | −0.0527 | 0.1963 | −0.0096 | −0.0393 |
| $S_D^{(A_1)}$ | −0.0521 | 0.0612 | 0.1132 | 0.0351 |
| $S_\gamma^{(A_1)}$ | −0.0337 | 0.0579 | −0.0148 | 0.1841 |
| | | X = Cl | | |
| $S_x^{(A_1)}$ | 0.2681 | 0.0040 | 0.0019 | 0.0144 |
| $S_r^{(A_1)}$ | −0.0295 | 0.1307 | −0.0184 | 0.0954 |
| $S_D^{(A_1)}$ | −0.0453 | 0.0372 | 0.1056 | 0.0770 |
| $S_\gamma^{(A_1)}$ | −0.0274 | −0.0897 | −0.0102 | 0.1723 |
| | | X = I | | |
| $S_x^{(A_1)}$ | 0.2682 | 0.0030 | −0.0009 | 0.0117 |
| $S_r^{(A_1)}$ | −0.0222 | 0.0993 | 0.0427 | 0.0289 |
| $S_D^{(A_1)}$ | −0.0437 | 0.1061 | −0.0661 | 0.0545 |
| $S_\gamma^{(A_1)}$ | −0.0279 | −0.0136 | 0.0039 | 0.1939 |

[a] $L$ is defined as the matrix relating the column vector of symmetry coordinates $S$ and the column vector of normal coordinates $Q$: $S = LQ$. [b] Subscripts to the normal modes designate the internal coordinates (see Figure 1) associated with the largest potential energy contribution.

$\bar{\alpha}'_{u_j}$ are given in Table XI. The Wolkenstein bond polarizability theory[26a] assumes that molecular polarizability derivatives do not depend on changes in bond orientation, *i.e.*, that $\bar{\alpha}'_u = 0$ for bending coordinates. This assumption has been found to hold quite well for a variety of molecules. For trimethylplatinum hydroxide, where $\bar{\alpha}'_Q$ values have been obtained for all four $A_1$ vibrations, it is possible to check this assumption by calculating $\bar{\alpha}'_{C-Pt-C}$. The resulting value is indeed very close to zero. For the chloride and iodide $\bar{\alpha}'_{C-Pt-C}$ was assumed to be zero for the calculation of the remaining three $\bar{\alpha}'_u$'s from the measurable $A_1$ modes.

For trimethylplatinum hydroxide the calculated value of $\bar{\alpha}'_{Pt-O}$ is negative. There is an inherent ambiguity in the sign of all normal mode polarizability derivatives, since they depend on the square roots of the Raman intensities. For the present set of molecules the signs of the roots were chosen to be positive; the signs of the associated eigenvectors are given in Table X. If the alternate root is taken for any of the $[(CH_3)_3PtOH]_4$ modes, the result is a larger negative

TABLE XI

BOND POLARIZABILITY DERIVATIVES AND BOND ORDERS FOR $[(CH_3)_3PtX]_4$

| | OH | Cl | I |
|---|---|---|---|
| $\bar{\alpha}'_{Pt-C}$, Å² | 2.03 ± 0.39[a] | 1.85 ± 0.30 | 1.86 ± 0.37 |
| $\bar{\alpha}'_{Pt-X}$, Å² | (−0.27)[b] | (0.25) | (0.63) |
| $\bar{\alpha}'_{Pt-Pt}$, Å² | 0.87 ± 0.25 | 0.61 ± 0.16 | (−0.24) |
| $\bar{\alpha}'_{C-Pt-C}$, Å² | (0.01) | (≡0) | (≡0) |
| $n/2$[c] (Pt–C) | 0.81 ± 0.16[d] | 0.74 ± 0.12 | 0.74 ± 0.15 |
| $n/2$ (Pt–X) | (∼0) | (0.08) | (0.12) |
| $n/2$ (Pt–Pt) | 0.12 ± 0.03 | 0.06 ± 0.02 | (∼0) |

[a] In cases where a single term $N_j\bar{\alpha}'_{u_j}l_{ji}$ in eq 2 clearly dominates the determination of a given $\bar{\alpha}'_{Q_i}$, the per cent error in $\bar{\alpha}'_{u_j}$ was taken to be the sum of the per cent error in $\bar{\alpha}'_{Q_i}$ and the total per cent contribution from the remaining $N_k\bar{\alpha}'_{u_k}l_{ki}$ terms. This procedure is based on our experience that in such cases the large $l_{ji}$ is well determined (insensitive to minor changes in the force field) while the smaller $l_{ki}$ are less certain (see text). The listed uncertainties are no doubt overly pessimistic. [b] For $\bar{\alpha}'_u$'s which could not be successfully approximated from a single nearly pure normal mode, the values are likely to be more sensitive to subtle features of the force field, and the estimation of uncertainties is not feasible. Such values are shown in parentheses (see text for further discussion). [c] Bond orders were calculated from eq 3, using the parameters: $X_{Pt} = 2.2$, $X_C = 2.5$, $X_O = 3.5$, $X_{Cl} = 3.0$, $X_I = 2.5$, $Z_{Pt} = 10$, $Z_C = 4$, $Z_O = 6$, $Z_{Cl} = Z_I = 7$. In view of the approximate nature of the theoretical model and the complexity of the problem, it seemed pointless to attempt to convert the Pauling electronegativities to valence-state electronegativities. [d] The errors here are the same per cent errors as in the $\bar{\alpha}'_u$ values; no uncertainties arising from the theoretical model or the choice of parameters are included.

value for $\bar{\alpha}'_{Pt-O}$ or negative values for one or more of the other $\bar{\alpha}'_u$'s. In a study of the thiocyanate ion,[27] Taylor, *et al.*, adopted a negative value for $\bar{\alpha}'_{C-S}$ in order to obtain a chemically reasonable value for $\bar{\alpha}'_{C-N}$. Ordinarily bond polarizability derivatives are assumed to be positive (the polarizability increasing as the bond is stretched).

The negative value obtained here for $\bar{\alpha}'_{Pt-O}$ arises from the fact that the calculated intensity contributions to the Pt–O stretching mode from the other internal coordinates, particularly Pt–C stretching with its large $\bar{\alpha}'_{Pt-C}$, exceed the observed intensity. While the intensity deficit is outside of experimental error, it is not clear what error limits to assign to the calculation. The force field used in the determination of the eigenvectors is not unique. Because the frequencies are already well calculated, modifications in the force field consistent with the observed frequencies are unlikely to produce major changes in the eigenvectors. However even small changes, while hardly affecting the *major* eigenvector elements, might produce an appreciable percentage change in the *minor* elements,[28] the kind which are responsible for the apparent intensity anomaly for the Pt–O mode. For example, if the eigenvector element for the Pt–C coordinate in the Pt–O mode were lowered from 0.0403 to 0.0111, a minor change in the *overall* eigenvector, the intensity anomaly would disappear and the calculated value of $\bar{\alpha}'_{Pt-O}$ would be zero. We conclude, therefore,

(26) (a) M. Wolkenstein, *Dokl. Akad. Nauk SSSR*, **30**, 791 (1941); (b) D. A. Long, *Proc. Roy. Soc., Ser. A*, **217**, 203 (1953).

(27) K. A. Taylor, T. V. Long, II, and R. A. Plane, *J. Chem. Phys.*, **47**, 138 (1967).

(28) D. A. Long, D. C. Milner, and A. G. Thomas, *Proc. Roy. Soc., Ser. A*, **237**, 197 (1956).

that the negative value of $\bar{\alpha}'_{Pt-O}$ may be an artifact and that the most that can be said about the Pt–O bond polarizability derivative is that it is not very different from zero. For the Pt–C and Pt–Pt modes in trimethylplatinum hydroxide, mixing is substantially lower, and the associated $\bar{\alpha}'_u$'s are well determined. The situation for the chloride is similar in that the Pt–C and Pt–Pt bond polarizabilities are much better defined than $\bar{\alpha}'_{Pt-Cl}$. For the iodide there is substantial mixing between the Pt–I and Pt–Pt modes, and the negative value of $\bar{\alpha}'_{Pt-Pt}$ can be ascribed to uncertainty from this source.

From bond polarizability derivatives one can estimate bond orders using the equation proposed by Long and Plane[25]

$$\bar{\alpha}'_u = \frac{2}{3}\frac{g\sigma}{Za_0}\left(\frac{n}{2}\right) r^3 \qquad (3)$$

where $n$ is the number of electrons in the bond, $r$ is the bond length, $a_0$ is the Bohr radius, $Z$ is the effective nuclear charge, $\sigma$ is the Pauling covalent bond character,[29] and $g$ is the strength of the $\delta$ function defining the interatomic potential. $Z$ is taken as the atomic number minus the number of inner-shell electrons, and $g$ is equated with the square root of the valence-state electronegativity on the Pauling scale, $X$.[29] For heteronuclear bonds the geometric average of the two $g/Z$ values is taken. While the theoretical basis for this equation is very approximate, it is nevertheless quite successful in predicting $\bar{\alpha}'_u$'s to within about 20% for a wide range of well-characterized molecules.[25]

Bond orders ($n/2$) calculated from eq 3 are listed in Table XI. The values for the Pt–C bonds are seen to be satisfactory, within 25% of the expected value of unity. For the Pt–X bonds the values are very much lower. This may be taken as an indication that these bonds are highly ionic. On this basis there seems to be a slight increase in covalency from X = OH to Cl to I. The $n/2$ values are even lower than those reported by Long and Plane,[25] for appreciably ionic $MX_4^{n-}$ species (M = Zn, Cd, Hg; X = Cl, Br), consistent with the expected weaker interaction with a triply bridging ligand.

The $n/2$ values for the Pt–Pt "bonds" are also quite low, implying that the metal–metal interaction is quite weak. This result is gratifying since *strong* metal–metal bonding is not expected in view of the relatively large Pt–Pt separations (see Table VI) and the stability of the Pt(IV) valence state ($d^6$). It is precisely the long internuclear distances which make Raman spectroscopy a sensitive probe for weak metal–metal interactions, because of the $r^3$ dependence of $\bar{\alpha}'_u$ (see eq 3). The $n/2$ values are seen to decrease smoothly from X = OH to Cl to I, the order of increasing Pt–Pt separation. For X = I, $n/2$ is indistinguishable from zero since all of the intensity of the Pt–Pt $A_1$ mode can be accounted for on the basis of mixing in of Pt–I stretching. The values for the hydroxide and chloride are similar in magnitude to corresponding values recently determined for $Bi_6(OH)_{12}^{6+}$, $Pb_4(OH)_4^{4+}$, and $Tl_4(OC_2H_5)_4$.[30]

It may be objected that evaluation of metal–metal interaction on the basis of the $\bar{\alpha}'_{Pt-Pt}$ values is impermissible because the latter depend on eigenvectors obtained from a force field in which metal–metal interaction is assumed, thereby making the argument circular. In fact the argument is not circular because the eigenvectors are not very sensitive to the choice of force field, as long as the alternative force fields attain a high level of accuracy in predicting the vibrational frequencies. In a test of this point, the spectra of $Pb_4(OH)_4^{4+}$ and $Tl_4(OC_2H_5)_4$ were recently analyzed[31] using on the one hand a force field with an M–M stretching force constant and on the other hand a force field with an M–O–M bending force constant. In each case the force constants were allowed to vary to obtain a least-squares fit to the frequencies. The resulting differences in the major eigenvector elements for the two different force fields amounted to less than 4% of their values. (The relative differences in the minor elements were substantially larger; see also the discussion above on the negative value for $\bar{\alpha}'_{Pt-O}$.) It seems very likely that similar results would be obtained for the $[(CH_3)_3PtX]_4$ species. Consequently, even if angle bending forces are used to account for the cluster *frequencies*, metal–metal interaction is necessary to account for the *intensities* of the $A_1$ cluster modes of the hydroxide and chloride in the Wolkenstein approximation, since this theory assumes that bending coordinates make no contribution. Alternatively, if the Wolkenstein theory is abandoned and it is assumed, for example, that for $[(CH_3)_3PtOH]_4$ Pt–O–Pt bending accounts for the cluster frequencies and the $A_1$ intensity, then a value for $\bar{\alpha}'_{Pt-O-Pt} \approx 0.3$–$0.5$ Å$^2$ is necessary. We know of no precedent for such a large derivative with respect to angle bending (compare the value of 0.01 Å$^2$ found for $\bar{\alpha}'_{C-Pt-C}$), and consider it particularly unlikely in view of the ionicity of the bonds forming the angle.

Returning to the question of the force constants for Pt–Pt stretching we note that the values are substantially higher than expected for the weak metal–metal interactions suggested by the Raman intensity data. For $[(CH_3)_3PtOH]_4$, $f_{Pt-Pt}$ is as large as $f_{Re-Re}$ (0.82 mdyn/Å)[32] in $Re_2(CO)_{10}$, a nonbridged complex with a genuine metal–metal bond. A similar situation was encountered for $Bi_6(OH)_{12}^{6+}$, $Pb_4(OH)_4^{4+}$, and $Tl_4(OC_2H_5)_4$. A possible explanation is that the metal–metal force constants are quite small and the restoring forces responsible for the cluster, or cage deformation, frequencies are primarily associated with M–O–M angle bending, despite the success of a metal–metal force constant in accounting efficiently for the recurrent simple cluster frequency ratios. However recent calculations have shown[31] that, for $Bi_6(OH)_{12}^{6+}$, $Pb_4(OH)_4^{4+}$, and $Tl_4(OC_2H_5)_4$, the requisite force field with

(29) L. Pauling, "The Nature of the Chemical Bond," Cornell University Press, Ithaca, N. Y., 1960, Chapter 3.

(30) C. O. Quicksall and T. G. Spiro, *Inorg. Chem.*, **9**, 1045 (1970).

(31) P. A. Bullner and T. G. Spiro, *Spectrochim. Acta*, in press.

(32) C. O. Quicksall and T. G. Spiro, *Inorg. Chem.*, **8**, 2363 (1969).

M–O–M bending is no more satisfactory, from a chemical point of view, than the one with M–M stretching. Instead of unaccountably large M–M stretching force constants, one is left with large and unaccountably variable M–O–M bending constants, as well as large and variable stretch–bend interaction constants.

Although the magnitude of the metal–metal force constants appears to be inconsistent with the observed intensities, the variations in the force constants are quite consistent with the bond order variations, for the $[(CH_3)_3PtX]_4$ molecules as well as for $Bi_6(OH)_{12}^{6+}$, $Pb_4(OH)_4^{4+}$, and $Tl_4(OC_2H_5)_4$.[30] In calculating $n/2$ for bonds between heavy-metal atoms, there is a considerable arbitrariness in allotting d electrons, as discussed previously.[30] Also, valence-state electronegativities are not known for these ions. With these qualifications, there appears to be a strong correlation between metal–metal force constant and bond order for all the bridged complexes except trimethylplatinum iodide, where the "simple cluster" model fails and consequently $f_{M-M}$ is not strictly comparable. The relevant data are summarized in Table XII. This behavior suggests that the intensity of the $A_1$ cluster mode and the restoring force for this vibration have a common origin, although the relationship between the two quantities is clearly different from the corresponding relationship for unbridged metal–metal systems (*e.g.*, $Mn_2(CO)_{10}$ and $Re_2(CO)_{10}$), in which similar force constants are associated with much larger bond orders.[30,32] We are unable at present to offer a plausible explanation of this phenomenon.

TABLE XII

$A_1$ CLUSTER FREQUENCIES, METAL–METAL FORCE CONSTANTS, AND BOND ORDERS FOR BRIDGED POLYNUCLEAR COMPLEXES

| Species | $\nu_{A_1}$(M–M), cm$^{-1}$ | $f_{M-M}$, mdyn/Å | $n/2$ | $r_{M-M}$, Å |
|---|---|---|---|---|
| $[(CH_3)_3PtOH]_4$ | 137 | 0.79 | 0.118 | 3.42 |
| $[(CH_3)_3PtCl]_4$ | 99 | 0.50 | 0.064 | 3.73 |
| $[(CH_3)_3PtI]_4$ | 88 | 0.49 | ~0 | 4.0 |
| $Bi_6(OH)_{12}^{6+}$ [a] | 177 | 0.97 | 0.061 | 3.71 |
| $Pb_4(OH)_4^{4+}$ [a] | 130 | 0.54 | 0.023 | 3.85 |
| $Tl_4(OC_2H_5)_4$ [a] | 102 | 0.27 | 0.016 | 3.83 |

[a] Intensity analysis from ref 30.

## Conclusions

The $[(CH_3)_3PtX]_4$ molecules extend the series of bridged polynuclear complexes for which there is evidence from Raman intensities for weak metal–metal interaction. The vibrational data for the hydroxide and the chloride are of unusually high quality, and the assignments are particularly clear-cut, because of the availability of single-crystal Raman spectra and because of the high symmetry of the crystals. Consequently, normal-coordinate analyses on these molecules are as free of ambiguity as can be expected for such complex structures.

The pattern that emerges from these measurements is very similar to that found previously for the oxygen-bridged complexes $Bi_6(OH)_{12}^{6+}$, $Pb_4(OH)_4^{4+}$, and $Tl_4(OC_2H_5)_4$. In every case there is a set of three low-frequency Raman bands whose frequency ratios correspond fairly closely to those expected in the simple cluster approximation for a tetrahedron, or octahedron, of like atoms. For this reason a force field involving a metal–metal stretching force constant provides an efficient fit to the spectra, whereas a force field involving instead an M–X–M bending force constant also requires a large stretch–bend interaction constant. While the efficiency of the fit does not prove the validity of a particular force field, strong evidence for metal–metal interaction is provided by the observation that in every case except $[(CH_3)_3PtI]_4$ the $A_1$ "metal–metal" Raman band is much stronger than the $A_1$ metal–bridging ligand mode. Therefore the metal–metal intensity cannot be explained by mixing in of the M–X mode. Since angle bending is not expected to contribute to the $A_1$ intensity, the only plausible mechanism to explain the intensity is metal–metal stretching.

Quantitative evaluation of the metal–metal bond polarizability derivatives and their transformation to bond orders *via* the Long and Plane equation show that the strength of the metal–metal interaction required to account for the Raman intensities is quite low. There are systematic trends in the calculated metal–metal bond orders. For the $[(CH_3)_3PtX]_4$ molecules they decrease with increasing Pt–Pt separation. For $Bi_6(OH)_{12}^{6+}$, $Pb_4(OH)_4^{4+}$, and $Tl_4(OC_2H_5)_4$ they decrease with decreasing nuclear charge on the metal ions. These trends are also reflected in the metal–metal force constants. On the other hand the force constants all seem to be about an order of magnitude higher than expected considering the weakness of the metal–metal interactions.

For the $[(CH_3)_3PtX]_4$ molecules the Pt–X force constants suggest that the bridging ligands experience a low effective nuclear charge on the platinum atoms, much closer to +1 than to +4. The polarizability derivatives indicate that the Pt–X bonds are highly ionic.

## Experimental Section

Trimethylplatinum hydroxide, chloride, and iodide were prepared by methods given in the literature[33] and purified by recrystallization from chloroform.

The large transparent single crystals needed for the Raman polarization measurements were obtained by slow evaporation of solvent from toluene or chloroform solutions at room temperature. A selected crystal of trimethylplatinum hydroxide was mounted on a goniometer head, and oscillation and Weissenberg X-ray photographs were used to determine the orientation of the crystal axes. The chloride crystal, which had the same morphology as the hydroxide crystal, was then oriented visually.

The Raman instrument used to record the spectra is described in detail elsewhere.[34] The 6328-Å line from a He–Ne laser and the 6471-Å line from an Ar–Kr laser (Coherent Radiation, Model 52) were used for excitation. The single-crystal spectra were obtained (6328-Å excitation) by attaching the goniometer head holding the crystal to a stand allowing rotation about the mounting axis. A polarization rotator provided control over the

(33) W. J. Pope and S. S. Peachey, *J. Chem. Soc.*, **95**, 571 (1909).

(34) R. E. Miller, D. L. Rousseau, and G. E. Leroi, Technical Report No. 22, ONR Contract 1858 (27), NR014-203, May 1967 (available from Defense Documentation Center, Cameron Station, Alexandria, Va. 22314).

direction of polarization of the incident beam, and a polaroid disk was used to analyze the scattered beam. In addition, a polarization "scrambler" was positioned at the monochromator entrance slit to eliminate anomalous intensity effects arising from dependence of instrument sensitivity on the polarization of light reaching the gratings. Solution spectra were obtained from saturated solutions of trimethylplatinum hydroxide and iodide in carbon tetrachloride and trimethylplatinum chloride in chloroform. Part of the Raman spectrum of the hydroxide was also investigated in benzene solution. Solutions were contained in a small multipass cell.

Relative intensities were obtained by measuring the areas of Raman lines and correcting the results for instrument sensitivity. For trimethylplatinum chloride, a Du Pont Model 310 curve resolver was used to analyze the complex 200–300-$cm^{-1}$ region.

Infrared spectra of the hydroxide and chloride were recorded on a Beckman IR-12 over the region 200–4000 $cm^{-1}$. Samples were examined as both KBr pellets and Nujol mulls held between polyethylene windows. For the iodide, the infrared spectrum of a Nujol mull was recorded on a Beckman IR-11 between 60 and 300 $cm^{-1}$.

**Acknowledgments.**—We wish to thank Miss B. Prescott of Bell Telephone Laboratories, Murray Hill, N. J., for recording the far-infrared spectrum of trimethylplatinum iodide and Mr. Aris Terzis for assistance in the mounting and orientation of single crystals.

---

CONTRIBUTION FROM THE DEPARTMENT OF CHEMISTRY, FLORIDA STATE UNIVERSITY, TALLAHASSEE, FLORIDA 32306

# Atomic and Molecular Spin–Orbit Coupling Constants for 3d Transition Metal Ions[1]

BY G. MATTNEY COLE, JR., AND BARRY B. GARRETT

*Received August 4, 1969*

Linear equations have been obtained relating the interelectronic repulsion parameters $F_2$ and $B$ and the spin–orbit coupling constant. The equations are obtained empirically from a least-squares fit of free-ion spectral data. Since reduction of the interelectronic repulsion parameters and the spin–orbit coupling constant for complexes relative to free-ion values may be treated as due to expansion of 3d radial wave functions, the equations may also be used to estimate effective spin–orbit coupling constants for complexes. Effective coupling constants, which compare favorably with those obtained from analyses of absorption spectra, are calculated for complexes of several metal ions.

## Introduction

The spin–orbit (SO) interaction in transition metal complexes makes important contributions to the splittings and intensities of electronic spectra,[2] zero-field splitting,[3] $g$ factors,[4] and line shapes[5] of electron resonance spectra and is related to the chemical shifts[6] and quadrupole splittings[7] observed in nuclear resonances for these systems. Unfortunately, the spin–orbit coupling constant is only rarely available as an experimental observable in a molecular environment. It is well known, however, that this constant is reduced from the free-ion value in complexes[4c] in similar fashion to the reduction of interelectron repulsion parameters (IRP).[8] These reductions may be explained by assuming that they result from radial expansion of the metal 3d atomic orbitals. Essentially the same results obtain by assuming that the charge on the metal in a complex is reduced relative to the free ion. Radial expansion of the metal ion 3d atomic orbitals thus provides an appropriate basis for correlation between the *effective* SO coupling constant and the interelectron repulsion parameters in both free atoms and complexes. This treatment should not be interpreted as a theoretical model. Rather it is an empiricism in which free-ion data for IRP's and SO coupling constants have been used with radial expectation values from self-consistent field wave functions to establish linear correlations for isoelectronic sequences and sequences of ions of a given nucleus. The empiricism is shown to be of predictive value for free ions and yields quite reasonable values for molecular SO coupling constants. We also note an interesting correlation between $\langle r^{-1} \rangle$ and the effective charge of the central metal ion in complexes which may be of value for comparison with the results of molecular orbital calculations.

## Procedure

Assuming a spherical Coulomb potential the spin–orbit interaction may be written[9,10]

$$V_{SO} = {}^1/_2\alpha^2 Z \sum_{i=1} \zeta_i(nl)\mathbf{l}_i \cdot \mathbf{s}_i \qquad (1)$$

(1) Presented in part at the 1968 Fall meeting of the American Physical Society, Miami Beach, Fla., Nov 25, 1968; G. M. Cole, Jr., and B. B. Garrett, *Bull. Amer. Phys. Soc.*, **13**, 1396 (1968).

(2) C. J. Ballhausen, "Introduction to Ligand Field Theory," McGraw-Hill, New York, N. Y., 1962, Chapter 6.

(3) A. Abragram and H. M. L. Pryce, *Proc. Roy. Soc., Ser. A*, **205**, 135 (1951); **206**, 164 (1951).

(4) (a) A. A. Misetich and R. E. Watson, *Phys. Rev.*, **143**, 335 (1966); (b) B. B. Garrett, K. DeArmond, and H. S. Gutowsky, *J. Chem. Phys.*, **44**, 3393 (1966); (c) R. Lacroix and G. Emch, *Helv. Phys. Acta*, **35**, 592 (1962).

(5) N. Bloembergen and L. O. Morgan, *J. Chem. Phys.*, **34**, 842 (1961).

(6) J. S. Griffith and L. E. Orgel, *Trans. Faraday Soc.*, **53**, 601 (1957).

(7) W. S. Childs and L. S. Goodman, *Phys. Rev.*, **170**, 50 (1968).

(8) C. K. Jørgensen, *Advan. Chem. Phys.*, **5**, 33 (1963).

(9) M. Blume and R. E. Watson, *Proc. Phys. Soc., London, Sect. A*, **270**, 127 (1963).

(10) E. U. Condon and G. H. Shortley, "The Theory of Atomic Spectra," 2nd ed, Cambridge University Press, Cambridge, England, 1963.